Delft University of Technology

Laser Swarm

Final Report

Design Synthesis Exercise

Authors:
S. Billemont
L.S. Boersma
B. Buyens
S.R. Finck
J.P. Florijn
T.C. Goossens
N.S. Oborin
A.J. Vorobiev
G.J. van der Wel
Z. Zhou

Tutor:
Ben Gorte

Coaches:
Prem Sundaramoorthy
Mathieu Willaert

June 14, 2010

Preface

This final document contains our evaluation of the Laser Swarm concept. Ten weeks have passed and we are finally ready to present our conclusions.

We did not, however, do everything by ourselves, and this is a good place to thank those who have been so kind as to give us some of their precious time.

First I want to mention professor Edoardo Charbon, who kindly explained and showed to us the workings of his Single Photon Avalanche Diode (SPAD)[1]: without his help we would be hopelessly in the dark on these fascinating devices. From this place I also want to thank professor Kourosh Khoshelham for helping us to some valuable material on remote sensing. I also want to thank Jasper Bouwmeester, who provided us with some helpful information on solar panel pricing.

And finally I thank our tutor, professor Ben Gorte, who was very generous to us with his time and has been very supportive of the entire project.

I hope you will have as much fun reading this report, as we had in making it!

Yours sincerely,

Co Florijn,
Chairman

---

[1]See [7, 98-105], [6] and [4]

Contents

List of Figures

List of Tables

List of Symbols

Symbol	Description	SI units
A	accuracy	rad
A	area	m^2
a	semimajor axis	km
C_D	drag coefficient	−
D	air drag	N
e	eccentricity	−
$\dot{e}$	time rate of change of the eccentricity	s^{-1}
g	gravitational acceleration	m/s^2
I_{rt}	round-trip interactivity loss	Watt
I_{sp}	specific impulse	s
i	inclination	rad
i_R	relative inclination	rad
$\dot{i}$	time rate of change of the inclination	rad/s
J_{ii}	inertia tensor for i	m^4
J_2	second zonal coefficient	0.001082645 −
J_3	third zonal coefficient	0.000002546 −
M_C	torque about c	N/m
m	mass	kg
m_f	fuel mass	kg
m_p	payload mass	kg
m_0	dry mass	kg
N	angular seperation	rad
n	nr of energy levels	−
n	mean motion	$7.292 \cdot 10^{-5}$ rad/s
n_e	refractive index	−
P	power	Watt
$p_{p,th}$	threshold power	Watt
R	mass ratio	−
R_C	radius of the orbit of the center of mass	km
R_E	earth equitorial radius	6378 km
s	variable in the Laplace equation	−
T	temperature	K
T_i	period of i	s
V	velocity	m/s
V_a	voltage at a	V
V_B	voltage at B	V
W	weight	N
η	pump efficiency	−
θ_i	angle w.r.t. rotation axis i	rad
θ_{man}	manoeuvre angle	rad
λ	wavelength	m
μ	gravitational constant of the Earth	$398600 \cdot 10^9$ m^3/s^2
ν	true anomaly	rad
ρ	density	kg/m^3
s	stimulated emission cross-section	m^2
t	upper level lifetime	s
ϕ	phase angle	rad
ϕ_R	relative phase angle	

Ω	right ascension of the ascending node	rad
$\dot{\Omega}_{J_2}$	rate of precession	rad/s
ω	argument of perigee	rad
$\dot{\omega}$	time rate of change of the argument of perigee	rad/s

List of Acronyms

ELS   Ensemble de Lancement Soyuz

EOL   End-of-Life

GLAS   Geoscience Laser Altimeter System

LEO   Low Earth Orbit

LiDAR   Light Detection And Ranging

RAAN   Right Ascension of the Ascending Node

SPAD   Single Photon Avalanche Diode

Abstract

In February 2010 the ICESat mission ended after 7 years of measuring ice sheet mass balance, cloud and aerosol heights, as well as land topography and vegetation characteristics using a space based Light Detection And Ranging (LiDAR) system. ICESat used only one of the possible approaches for LiDAR, namely the use of a high energy laser and a large receiver telescope. The other approach is using a high frequency, low energy laser and a single photon detector. The advantage of the latter approach is that it has a much lower mass, but it is uncertain if even a single photon per pulse reaches the receiver. One possible solution could be to use a swarm of satellites around the emitter, each equipped with a single photon detector. However, the technical feasibility of this concept has not yet been proven.

This report briefly highlights different ways in which such a mission could be accomplished, and then decides what way will be the most likely to succeed.

Chapter 1

Introduction

In February 2010 the ICESat mission ended after 7 years of measuring ice sheet mass balance, cloud and aerosol heights, as well as land topography and vegetation characteristics. To do all this, ICESat had only one instrument on board: a space based LiDAR system (Geoscience Laser Altimeter System (GLAS)), allowing for an unprecedented 3D view of the Earth's surface and atmosphere. The laser lifetimes, however, were severely limited because of manufacturing errors in one of the laser components.

ICESat followed only one of the possible approaches for LiDAR, namely the use of a high energy laser and a large receiver telescope. The other approach is using a high frequency, low energy laser and a single photon detector. The advantage of the latter approach is that it has a much lower mass, but it is uncertain if even a single photon per pulse reaches the receiver. One possible solution could be the use of a swarm of satellites around the emitter, each equipped with a single photon detector. However the technical feasibility of this concept has not yet been proven.

In this mid term review some options for this concept are proposed and traded off so as to find the best fit for the mission. This tradeoff is what the bulk of this report is about. Also described are the workings and results from the simulator, as well as the project and risk management. Chapters on operation and logistics, stability and control and sustainability are included too.

Chapter 2

Launch and Astrodynamic Characteristics

This chapter explains the characteristics of the launch and space segments of the mission. Section 2.1 describes the three main characteristics of bringing the swarm into the orbit: launch vehicle, launch location and orbit insertion. Section 2.2 discusses all the aspects of the constellation and its configuration, and delves into estimations of ΔV and needed propellant. Finally, section 2.3 deals with the hazardous space environment and ways of protecting the satellites against it.

2.1 Launch Segment

The launch segment of the mission includes the selection of the launch vehicle, the launch location and the procedure of inserting the satellites into their respective orbits. The following subsections discuss all of these aspects.

2.1.1 Launch Vehicle

The costs of launch vary greatly between different vehicles. Table 2.1 on page 2 lists approximate total launch costs of respective platforms. The prices are given in Fiscal Year 2000 dollars for consistency.

Platform	Operator	Price (FY00$m)
Ariane V	ESA	97.96
Soyuz	Starsem or Arianespace	8.16 - 22.1
Vega	European and Italian SA	15.1
Falcon 1E	SPACEX	8.89
PSLV	ISRO	13.88 - 16.33
Rokot	Eurokot	9.8 - 11.4

Table 2.1: Estimated price comparison of different launch vehicles. *Source: various.*

Based on the information in the above table it is possible to single out a few platforms which will be

affordable for the purpose of this feasibility study. The values represent the total launch segment costs. The Ariane V launcher is the most expensive option by far and would push the budget quite heavily, with an estimated cost of launch almost half of the total budget. However the payload capabilities of the Ariane V launcher far outweigh that of all other platforms, thus making it possible for a combined launch with other satellites, leading to shared costs. This however could jeopardize the mission in the sense that it becomes secondary priority. If that happens, the constellation would have have have higher requirements for orbit acquisition: an extra booster stage or higher onboard fuel capacity for the altitude and/or plane shift, which is not feasible. The Ariane V is therefore an unsuitable platform for this project.

The rest of the launchers can be analyzed with respect to reliability. All of the launch vehicles have been tested, with the exception of the Vega system, which is yet to make its maiden flight. The Vega is therefore not suitable for the analysis at this time. It is for this reason that the project will no longer consider this system at all. However, better data should be available in the near future which should allow for the Vega platform to be reevaluated.

The same goes for the Falcon - 1e system. The launcher is still under development. Furthermore, the predecessor of the 1e system is the Falcon - 1, which out of total of five launches only had two successful, fails to make a favorable impression.

Table 2.2 on page 3 shows some reliability statistics for the remaining 3 vehicles.

Platform	Total No. of Launches	Total Failures	Reliability	No. of Successful Launches Since Last Failure
Soyuz	1754	88	95%	57
PSLV	16	1	94%	15
Rokot	17	2	88%	6

Table 2.2: Reliability figures for several launch vehicles. *Source: various.*

The Soyuz launch vehicle presents itself as the most reliable platform, with a track record that far surpassed all other options. This launch vehicle will be the one considered for this project. In the next section, its payload capabilities are discussed.

2.1.1.1 Soyuz LV Payload Capability Analysis

There is a large selection of Soyuz vehicles available for consideration. For the purpose of this project, the newest modification - Soyuz-ST will be used. This vehicle is part of the Soyuz-2 family, which are technologically superior to the older Soyuz-U and U2 launchers. An illustration and technical parameters of the Soyuz-ST can be found in Appendix A on page 29 [1].

An estimation of mass performance for the launch vehicle can be seen in figure 2.1 on page 4.

The payload mass data provided in [1] is estimated, yet is good enough to have a reasonable idea about the maximum mass. The Soyuz-ST is able to launch roughly a maximum of 5000 kg into a 500km orbit. This is well above the design mass of the formation thus will allow for further considerations of joint launches (as long as the swarm mission is considered to be the primary payload) and thus spread launch costs.

The available volume in the Soyuz-ST Fairing can be seen in figure 2.2 on page 5.

The dimensions of the fairing are visibly too large and there is no possibility of using a different one, however that leaves a lot of possibilities for different designs of release adapters to adapt to the unique sequence of separation upon orbit injection. Again, the possibility of taking other small satellites along on
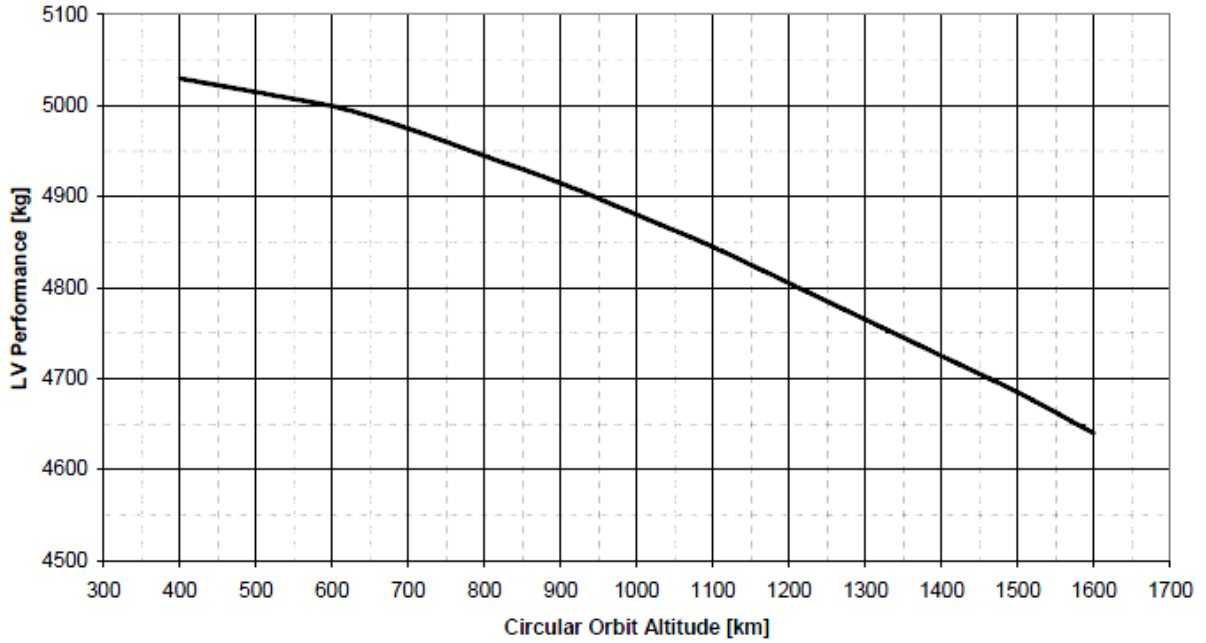
Figure 2.1: Mass performance of the Soyuz-ST for circular Orbits. *Source: [1].*

the same launch arises. The dual launch configuration shown in the previous figure is the one being considered for the launch.

The choice of the Soyuz brings forth one more advantage: the use of a unique orbit insertion booster, the Fregat. This final stage will allow for minimization of fuel on the satellite as all orbit insertion maneuvers can be done using the Fregat. The Fregat stage has been designed to handle 20 individual burns.

2.1.1.2 Vibrational Analysis

HERE ADD VIBRATION ANALYSIS

2.1.2 Launch Site

The selection of the launch site relies on several factors:

- Availability of attainable inclinations from launch.
- Compatibility with the launch vehicle.
- Accessibility and cost.
- Security and political reasons.

The first factor is crucial. It is paramount that the satellites are injected into their final inclinations at launch and do not have to perform any inclination change maneuvers, which require a substantial ΔV. With this in mind choosing a launch site closer to the equator is necessary. Launch sites at higher latitudes
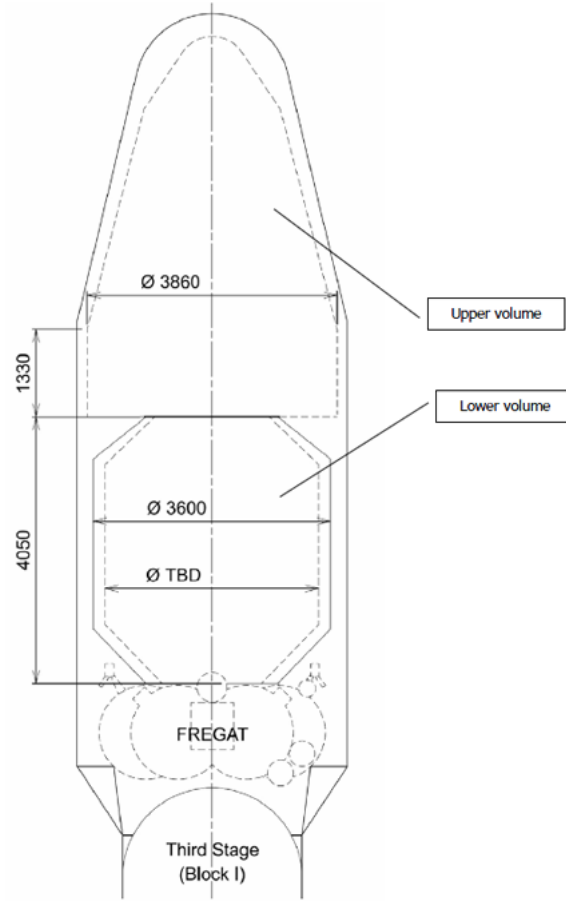
Figure 2.2: Fairing volume of the Soyuz-ST launch vehicle. Here shown in dual launch carrying configuration. *Source: [1].*

would need to sacrifice velocity and thus payload mass because of their location. Table 2.3 on page 5 shows a number of possible launch sites and their locations [9]. The list contains only the sites compatible with the Soyuz-ST launch vehicle. Furthermore, in figure 2.3 on page 6, the same sites are indicated with their respective authorized inclination ranges.

Launch Site	Operator	Latitude (deg min)	Longitude (deg min)
Baikonur LC-31/6	Russia (Starsem)	45 54 N	63 18 E
Plesetsk LC-43	Russia (Starsem)	62 48 N	40 24 E
Guiana Space Centre ELS	CNES/Arianespace	5 18 N	52 50 W

Table 2.3: Available launch sites for the Soyuz-ST. *Source: [9].*

Even though all the above sites allow inclinations of 85 degrees, it is still preferable to select a site closer to the equator in order to utilize the full effect of Earth's rotation and lower the launch costs. With this in mind, the Guiana Space Centre is selected to be the preferable location for launch.

Figure 2.3: Launch site locations and allowable inclinations for the Soyuz-ST. *Sources: [8] and [5].*

The Ensemble de Lancement Soyuz (ELS) in Kourou, Guiana is currently being finalized and should accommodate its first Soyuz launch in 2010 [2].

A typical launch profile of the Soyuz launch vehicle from Kourou is shown in figure 2.4 on page 7. The first three stages of the vehicle are used propel the payload and the Frigate booster to a circular orbit at around 200 km. After separation (stage 6 on the figure), the Fregat initiates the first orbit injection burn to bring the satellites to the appropriate orbits.

With this information it is possible to further calculate some important launch parameters:

- The inertial velocity of the launch site is given by:

$$V_L = (464.5)cosL \tag{2.1}$$

  where L is the site latitude. For the case of Kourou the inertial velocity is 462.51 m/s.

- The launch azimuth in inertial frame of reference is given by:

$$A_{Z_I} = arcsin(\frac{cosi}{cosL}) \tag{2.2}$$

  and is equal to 5.022 degrees for this launch.

- The launch azimuth corrected for the Earth's rotation, is given by:

$$A_Z = arctan(\frac{V_0 sinA_{Z_I} - V_{eq}cosL}{V_0 cosA_{Z_I}}) \tag{2.3}$$

  where V_0 is the orbital velocity reached by the launcher before separation and the first burn of Fregat upper stage (see above, around 7.784 km/s), V_{eq} is the velocity of the Earth's rotation at the equator - 464.5 m/s. Thus the corrected launch azimuth becomes 1.61 degrees.
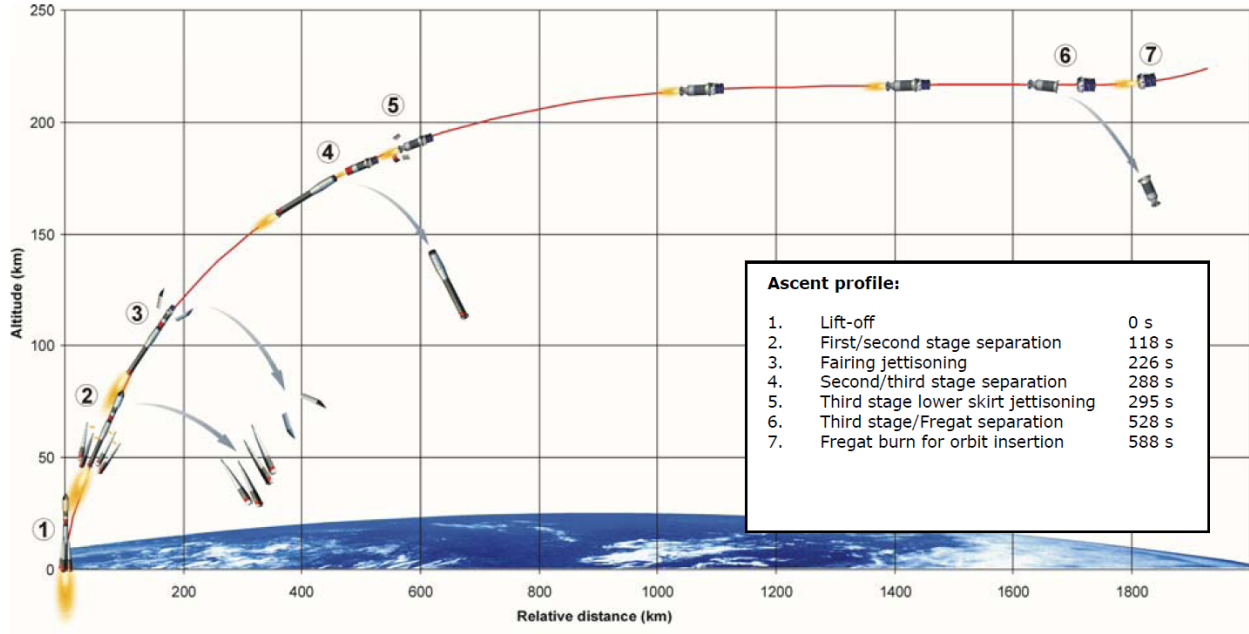
Figure 2.4: Launch profile of the Soyuz LV from Kourou. *Sources: [1].*

- The required launch velocity is calculated to be 7.76 km/s which means that due to Earth's rotation 26.8 m/s are saved.

Furthermore the region is politically stable and the launch site is under the protection from the French government and other security forces. All safety procedures are kept to the highest of standards and the spaceport is easily accessible by air or sea [1].

2.1.3   Orbit Insertion

The orbit insertion is separated into two distinct stages: primary orbits and secondary orbits. The primary orbits are located at an altitude of 500 km and contain the emitter and four initial receivers. The secondary orbits are located at a slightly different altitude of 525 km and contain the auxiliary receivers intended for replenishment.

The configuration of the primary orbits is discussed in section 2.2.3 and an image of the formation can be seen in figure 2.11 on page 20. The release sequence and the important parameters are as follows (for satellite and orbit numbers please refer to figure 2.11):

1. The Fregat is injected in Orbit 1.

2. The ascending intersection of Orbit 1 and Orbit 2 is reached at a latitude of 85° and a longitude offset (from the ascending node of Orbit 1) of 88.91°. At this point the Fregat should be orientated in the direction of Orbit 2 and separate Rec 2. The separation ΔV that the adapter should produce is calculated using:

$$\Delta V = 2V_i sin\frac{\alpha}{2} \tag{2.4}$$

where V_i is the orbital velocity (7.612 km/s) and α is the relative inclination (2.17°, see section 2.2.3) [3]. The ΔV is calculated to be 289.63 m/s.

3. As the Fregat crosses the descending node and approaches the second plane intersection of the orbit, it does not need to change orientation (Orbit 3 intersects in the same direction on the descent phase as Orbit 2 does on the ascent phase). At the intersection Rec 1 is separated with a ΔV of 289.63 m/s. This is a very large value thus the method of deployment should be thoroughly investigated in further design.

4. After this the Fregat again aligns with the velocity vector of Orbit 1.

5. The Frigate should inject itself into a drift orbit with a negative drift rate of no less then 9.19 deg/orbit and re-injected back to Orbit 1 after traveling $90 + \Delta\phi/2 = 90.09505$ degrees. This will bring the launcher 2.3 degrees behind the final emitter position, or 0.12 degrees behind Rec 4.

6. At this point the remaining three satellites: Rec 3, Base and Rec 4 should be put into drift orbits by the attachment mechanism in order to acquire the 2.18 degree orbital separation. The exact order and timing can be designed and adjusted accordingly.

After this, the satellites can be considered to be in their orbits. The Fregat can start the burn to insert into the secondary orbits. Once the altitude of 525 km is reached the Fregat performs a plane shift to change its Right Ascension of the Ascending Node (RAAN) to approximately 10 degrees behind that of the primary orbit. The exact angle has to be carefully acquired through careful modeling of differential node precessions as the satellites decay. The general idea is that the secondary satellites should have the correct RAANs by the time they decay to arrive in the right position with respect to the emitter. The formation in the secondary orbit is the same as in the primary orbits minus the emitter, thus similar maneuvers have to be performed.

2.1.4 Launch Date

The launch date is dominated by development times and lifetime considerations. The satellite orbit decay is and thus lifetime is a function of atmospheric density. The density is, in turn, a function of the solar activity. The number of sun spots on the surface of the sun rises and falls every eleven years. The measurements are commonly represented in 10.7cm radio flux intensities. Figure 2.5 on page 9 presents a projection for the next 10 years.

In order to provide the longest possible lifetime for the mission it is essential that the launch is timed in such a way that the satellites are in orbit most of the time during solar minimum. For this reason a launch on March 1st 2017 is planned. This also gives enough time for development and production. For further information on the timeline, please refer to section **??**.

2.2 Space Segment

This section covers the astrodynamical characteristics of the mission. Emitter orbit is covered first, then in section 2.2.2, all receiver orbits are examined. The formation and its properties are discussed in section 2.2.3. Collision avoidance is described in section 2.2.5 and, finally, section 2.3 covers the orbital environment and whether the mission is going to be heavily affected by it.
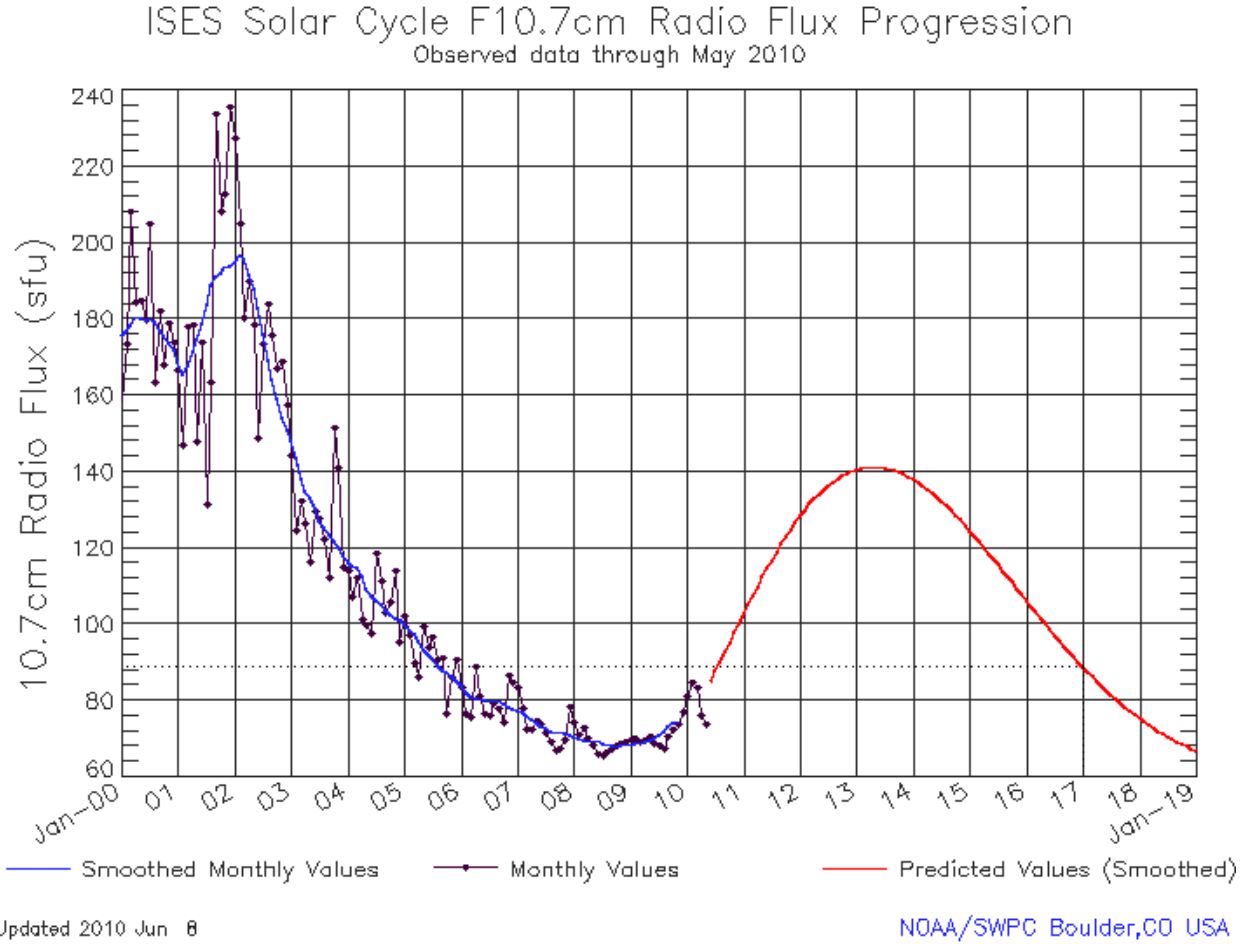
Figure 2.5: Solar activity projection up to 2019. *Source: NOAA/Space Weather Prediction Center.*

2.2.1 Emitter Orbit

2.2.1.1 Orbital Parameters

The emitter satellite is injected into a circular orbit at an altitude of 500 km. The eccentricity is frozen at 0. Inclination is chosen to be 85 degrees, as this allows access to polar areas, which are places of interest for the mission. Furthermore, the inclination provides an inherent relative phase for the crossing orbits. The Right Ascension of the Ascending Node can be chosen arbitrary for the start of the mission, as no specific target is assumed for the mission. For consistency, in all following discussions it is assumed to be 0 degrees. The same goes for the Argument of Perigee and the True Anomaly. As the orbit is circular, these values are not really relevant. The emitter satellite acts as the reference for all the receivers.

The orbit is non-sunsynchronous and does not have a specific repeat track. This allows for larger coverage of the Earth.

Figure 2.11 on page 20 shows the emitter satellite (labeled as Base) in Orbit 1.

A few basic properties of this orbit can be derived and are shown in table 2.4 on page 10. All the values were generated with the help of [9], [3] and [8].

Parameter	Symbol	Value	Unit
Altitude	h	500	[km]
Semi-major Axis	a	6871	[km]
Eccentricity	e	0	[-]
RAAN	Ω	0	[deg]
Period (mins)	P	94.6135	[mins]
Revolutions per day		15.2198	[revs/day]
Angular Velocity	n	3.805	[deg/min]
Circular Velocity	V	7.6127	[km/s]
Max. Eclipse	T_e	35.75	[mins]
Node Spacing		23.72	[deg]
Node Precession	$\dot{\Omega}$	-0.6667	[deg/day]

Table 2.4: Orbital properties of the emitter satellite.

2.2.1.2 Orbit Decay

Atmospheric drag is by far the most relevant perturbation for Low Earth Orbit (LEO) satellites that cause loss of altitude and thus decays the orbit. It directly relates to mass as it influences the amount of fuel required to maintain the orbit, where as the mass influences the rate at which the orbit decays. Altitude selection relies heavily on estimation and analysis of drag data as for longer mission times, higher altitudes are preferred, while optical instruments prefer lower altitudes for increased accuracy.

The drag that the satellite experiences due to atmospheric density is described by the following formula:

$$D = -\frac{1}{2}C_D\rho V^2 A \tag{2.5}$$

It follows that orbital parameter changes (semi-major axis, period and velocity respectively) per orbit are calculated using the following equations (assuming negligible eccentricity):

$$\Delta a = -2\pi \left(C_D \frac{A}{m} \right) \rho a^2 \tag{2.6}$$

$$\Delta P = -6\pi^2 \left(C_D \frac{A}{m} \right) \rho \frac{a^2}{V} \tag{2.7}$$

$$\Delta V = \pi \left(C_D \frac{A}{m} \right) \rho a V \tag{2.8}$$

The fundamental problem with accurately predicting effects due to atmospheric drag is twofold: firstly it is very hard to predict the satellite's ballistic coefficient:

$$\frac{m}{AC_D} \tag{2.9}$$

Even with a well known mass to area ratio, the coefficient of drag can be highly variable, highly dependent on the shape of the satellite and its orientation with respect to the velocity vector. It is usually determined in laboratory conditions. For the orbit decay analysis the following equation for the coefficient of drag was used:

$$C_D = \alpha C_{DS} + \beta C_{DD} \tag{2.10}$$

where C_{DS} is the specular coefficient of drag, C_{DD} is the diffuse coefficient of drag, α and β are component fractions which are determined experimentally. The specular coefficient of drag is usually predominant. In reality this drag coefficient changes. The cross-sectional area normal to the velocity vector can also vary for the swarm satellites if the whole platform is reoriented for instrument pointing. These parameters were adjusted in such a way that a final average C_D of 2.22 for the emitter as well as the receiver was achieved. This is a value which is very commonly used in space mission design.

The cross-sectional area of the satellite perpendicular to the velocity vector for a sample period of 6 hours can be seen in figure 2.6 on page 11. The graph was generated using the correct geometry of the satellite simulated in the Satellite Tool Kit$^{\text{TM}}$software, issued by AGI, Inc. The software also computes the mean area - 1.045948 m^2. This will be the area used for lifetime analysis. The mass used is final estimated satellite loaded orbit mass from section **??**. It is computed to be 22.87 kg/m^2. This is well within the normal range for regular satellites [9].
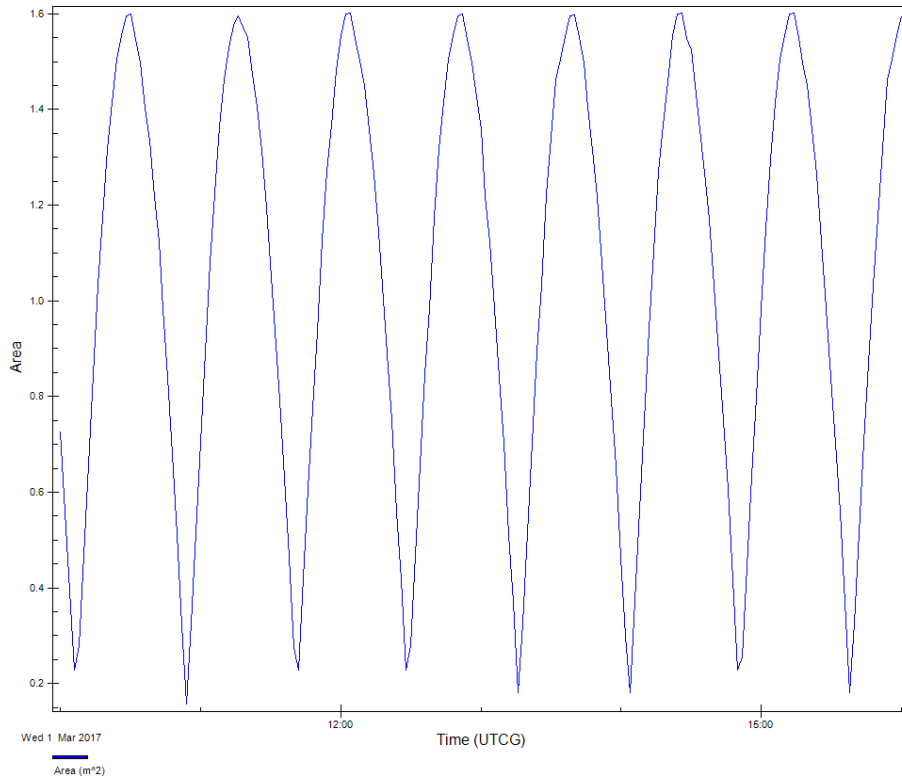

Figure 2.6: Simulated cross-sectional surface area of the emitter satellite perpendicular to velocity vector.

The second reason drag calculations are so unreliable, is because air density at any altitude is highly variable. Raising air density is primarily connected with solar activity. As solar activity increases every 11 years the atmosphere heats up. Contrary to conventional gas laws that would dictate a fall in density as the gas expands, the atmosphere simply rises, increasing density at higher altitudes. This was previously discussed in section 2.1.4.

The density difference during maxima and minima for different altitudes is shown in figure 2.7 on page

12. Depending on the altitude, the density could vary for up to a whole order of magnitude between the minimum and maximum.
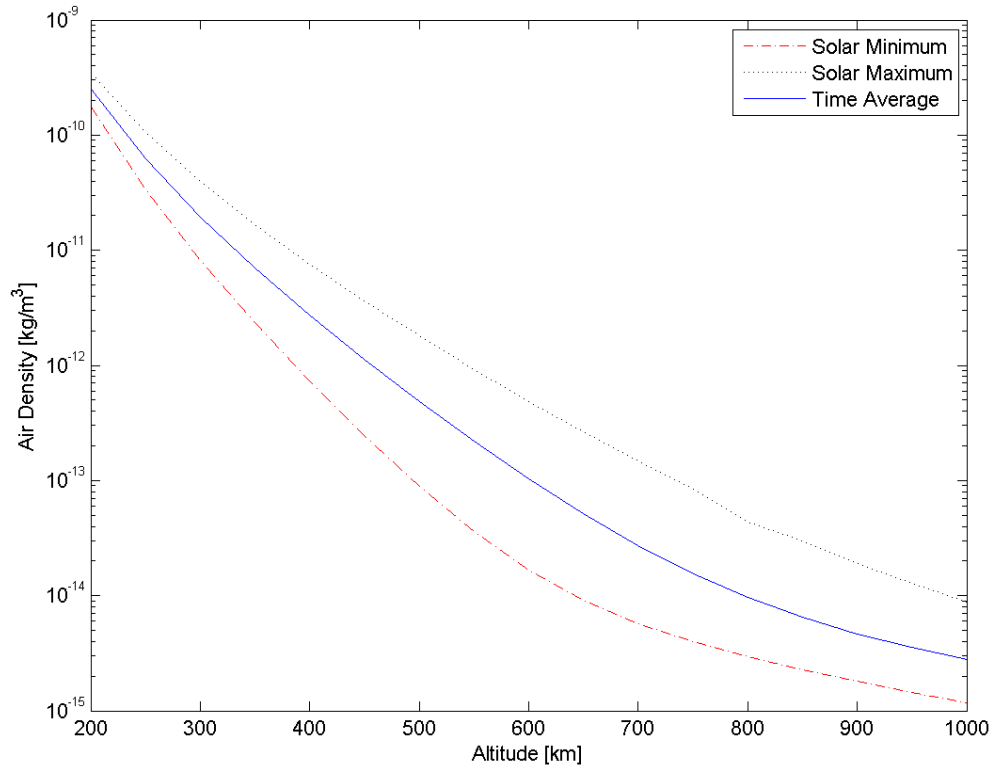

Figure 2.7: Air density vs. orbit altitude for different solar cycle stages.

The orbit lifetime simulation was produced using the software package Satellite Tool Kit[TM]and can be seen in figure 2.8 on page 17.

The simulation performs orbit propagation up to the J_4 factor and uses the MSIS-86 Thermospheric Model for atmospheric density calculation. In addition it takes into account solar radiation pressure with an average sun exposed area of 0.84 (this area is also estimated from the satellite model simulations).

It is obvious from the previous figure that, unmaintained, the orbit would totally decay in 4.8 years. Another notable time is the point at which the emitter passes the 450km altitude. This occurs at approximately 3.4 years after mission start. This is the altitude that will be considered as the absolute floor and will be used to approximate the altitude of the secondary satellite orbits.

2.2.1.3 Estimation of ΔV

In order to properly estimate the mass of the propellant required for the mission all maneuvers have to be taken into account. Every maneuver requires a certain velocity change in a specified direction. During its mission, the emitter satellite will perform the following maneuvers:

- A phase change slowdown. As the satellite was released from the booster vehicle, it was injected into a

drift orbit in order to separate into a certain phase shift. Once this phase shift is achieved, the satellite needs to perform a boost to bring itself back into the circular orbit. This ΔV is equal and opposite to the ΔV induced by the release mechanism. This ΔV is calculated using the following equation:

$$\omega_{drift} = (1080)\frac{\Delta V}{V} \tag{2.11}$$

where ω_{drift} is the drift rate given in deg/orbit. For the emitter to return out of its drift orbit in 90 degrees, this maneuver requires a ΔV of 64.8 m/s.

- A boost to change the altitude from 450 km to 500 km after approximately 3.4 years in orbit. This maneuver is performed using a simple Hohmann transfer orbit and will require two burns. A simple transfer calculation is completed using the following method [3]:

$$V_{450} = \sqrt{\frac{GM}{a_{450}}} = 7.6405 km/s \tag{2.12}$$

$$V_{500} = \sqrt{\frac{GM}{a_{500}}} = 7.6127 km/s \tag{2.13}$$

$$a_{ellipse} = \frac{a_{500} + a_{450}}{2} = 6853 km \tag{2.14}$$

$$V_p = \sqrt{\frac{2GM}{a_{450}} - \frac{GM}{a_{ellipse}}} = 7.6544 km/s \tag{2.15}$$

$$V_a = \sqrt{\frac{2GM}{a_{500}} - \frac{GM}{a_{ellipse}}} = 7.5988 \tag{2.16}$$

$$\Delta V_1 = 1000(V_p - V_{450}) = 13.9237 m/s \tag{2.17}$$

$$\Delta V_2 = 1000(V_{500} - V_a) = 13.8984 m/s \tag{2.18}$$

$$\Delta V = \Delta V_1 + \Delta V_2 = 27.8221 m/s \tag{2.19}$$

Thus the required ΔV for the Hohmann transfer is 27.8 m/s.

- A deorbit burn to take the satellite down to comply with sustainability requirements. This ΔV is approximated by the following equation [8]:

$$\Delta V_{deorbit} \approx V\left[\frac{0.5(H_i - H_e)}{2R_E + H_i + H_e}\right] \tag{2.20}$$

where H_i is the initial altitude, H_e is the reentry altitude and R_e is the Earth's radius. Using the initial altitude of 500 km and a reentry altitude of 50 km, the ΔV is calculated to be 128.73 m/s. This is a very large value and in reality can be scaled down by considering a lower initial altitude (500 km is asumed in this analysis due to the consideration that a satellite might become disfunctional at the beginning at the mission and would need to be brought down) and a higher final reentry altitude (which is arbitrary).

- The final consideration is the orbit injection accuracy of the Soyuz launch vehicle. The manufacturer states an inclination accuracy of 0.033 degrees for a 1000 km altitude orbit [1]. For the purposes of this analysis, an accuracy of 0.03 degrees is used. The following equation is used to estimate the ΔV needed to correct this error:

$$\Delta V_{planechange} = 2V_i sin\frac{\alpha}{2} \tag{2.21}$$

where V_i is the initial orbital velocity. The final ΔV is 3.99 m/s.

No ΔV is required for stationkeeping as the emitter will be allowed to decay naturally while the receivers will have to perform relative stationkeeping. Furthermore, the Soyuz launch vehicle can have a initial delivery altitude error. This is not considered, since it is assumed that as long as the constellation is delivered on the same altitude, no correction will be required and the lifetime of the mission will not be jeopardized.

The total ΔV required for the emitter is calculated to be approximately 225.38 m/s.

2.2.2 Receiver Orbits

2.2.2.1 Orbital Parameters

Unlike the emitter, the receiver satellites are placed in six different orbits and has to be designed to be able to handle all orbits and yet all the satellites have to have the same mass configuration at all times.

The orbits are divided into primary and secondary. The primary orbits are shown in figure 2.11 on page 20. Receiver 1 is located in Orbit 3 which has all the same orbital characteristics of Orbit 1 as described in section 2.2.1.1 with the exception of its RAAN having a value of +2.18 degrees. This is the maximum angle of separation and is derived from the requirement of a laser reflection angle of 30 degrees. Receiver 2 in Orbit 2 on the other hand has a RAAN of -2.18 degrees. Both of these receiver satellites pass their ascending nodes at the same time as the emitter satellite. The reason for this is that the inclination of the orbits induces a relative phase between the satellites which is favorable for collision avoidance.

Receivers 3 and 4 are placed on the same orbit as the emitter. Receiver 3 travels with a positive phase offset of 2.18 degrees in front of the emitter, while the latter is trailing the emitter at the same offset.

All orbital velocities and other parameters are identical to those described in section 2.2.1.1.

The secondary orbits are designated 1S,2S and 3S, and are arranged in a similar manner while having an orbital altitude of 525 km. Receivers 1S, 2S, 3S and 4S also correspond in their arrangement to their primary counterparts.

Parameters of the secondary orbits that are different to those of the primary are shown in table 2.5 on page 14.

Parameter	Symbol	Value	Unit
Altitude	h	525	[km]
Semi-major Axis	a	6896	[km]
Period (mins)	P	95.1298	[mins]
Revolutions per day		15.1372	[revs/day]
Angular Velocity	n	3.7843	[deg/min]
Circular Velocity	V	7.6127	[km/s]
Node Spacing		23.85	[deg]
Node Precession	$\dot{\Omega}$	-0.6584	[deg/day]

Table 2.5: Orbital properties of the secondary orbits (only the parameters different to those of the primary orbits are shown).

The initial RAANs are yet to be determined and a very complex model is required to account for differential precessions between the primary and secondary orbits. This is crucial in order for the secondary constellation to arrive in the right place with respect to the emitter. The calculations though fall out of the scope of this investigation.

2.2.2.2 Orbit Decay

The orbit decay analysis is done is a manner identical to that described in section 2.2.1.2. The final loaded mass of all the primary receiver satellites should be the same as the final orbits are established in order to decay at the same rate. The mean drag area estimated with the STK$^{\text{TM}}$software is 0.3 m^2. The loaded mass is taken from section **??**. The area exposed to sun (for solar pressure) is calculated to be 0.25 m^2. The ballistic coefficient then becomes 22.40 kg/m^2, which is extremely close to that calculated for the emitter satellite, certainly within the margins at this point in the design. This is key to maintaining the constellation. The final design of all the satellites should ensure they decay in absolutely the same manner.

The results of the decay simulation can be seen in figure 2.10 on page 19. They are virtually the same as the decay shown in figure 2.8.

The decay rate of secondary satellites is shown in figure 2.10 on page 19. The actual altitude was iterated in order to see that the receivers would decay to 500 km in mid August 2020. In reality the secondary satellite will have to take 0.3 kg of fuel less then the primary (at the expense of less fuel available for the deorbit maneuver) as the emitter satellite would have lost 27.8 m/s worth of propellant after the Hohmann transfer back to 500 km. This will ensure the same decay rate of the secondary leg of the mission.

2.2.2.3 Estimation of ΔV

During the mission different receiver satellites will require different ΔV. The main concern is to equalize them as the final orbits are established. The differences are only different due to different phase shifts needed and different orbital velocities.

The satellites will need to perform the following maneuvers:

- A phase shift maneuver similar to the one described in section 2.2.1.3. For this maneuver different drift rates are required for the satellites. Receivers 1 and 2 will need a ΔV of 32.42 m/s (drift rate assumed to be half an orbit). Receiver 3 would require 31.58 m/s, but would require a whole orbit to establish its position. Receiver 4 would require a mere 0.85 m/s.

  The secondary orbit satellites have a different circular velocity thus also have different ΔV's. Receivers 1S and 2S require 32.37 m/s. Receiver 3S needs 31.52 m/s, and finally, Receiver 4S requires 0.84 m/s.

- The deorbit maneuver will require the same ΔV for all primary satellites and is also equivalent to the that of the emitter - 128.73 m/s. The secondary satellites will require 27.8 m/s less (100.93 m/s in total) as explained earlier.

- The correction for orbit insertion is identical for all primary satellites - 3.99 m/s (see section 2.2.1.3). Secondary satellites need a ΔV of 3.98 m/s. This difference is neglegiable.

The total ΔV for each receiver satellite is computed in table 2.6 on page 15.

	R1/R2	R3	R4	R1S/R2S	R3S	R4S
Phase shift	32.42	31.58	0.85	32.37	31.52	0.84
Deorbit	128.73	128.73	128.73	100.93	100.93	100.93
Inclination Correction	3.99	3.99	3.99	3.98	3.98	3.98
Total	165.14	164.3	133.57	137.28	136.43	105.75

Table 2.6: Total ΔV for individual receiver satellites. Values are given in m/s.

The largest ΔV (i.e 165.14 m/s) was used for propulsion system design.

Again no numbers are specified for stationkeeping. This topic is elaborated on in section 2.2.4.
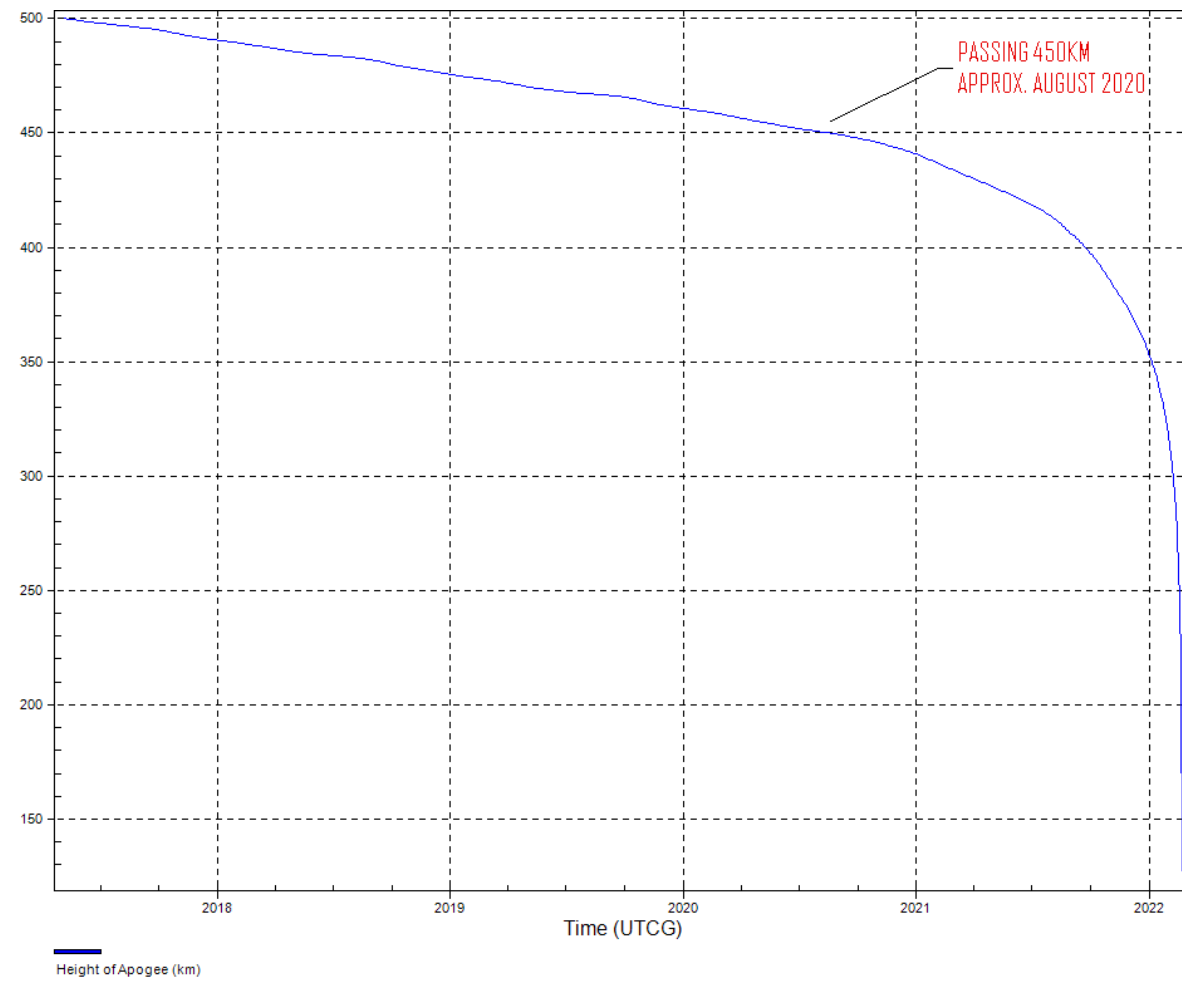
Figure 2.8: Emitter satellite orbit decay with an assumed mission start in March 2017. Values used: $C_D = 2.22$, mass = 53.1 kg, Area = 1.046 m^2.
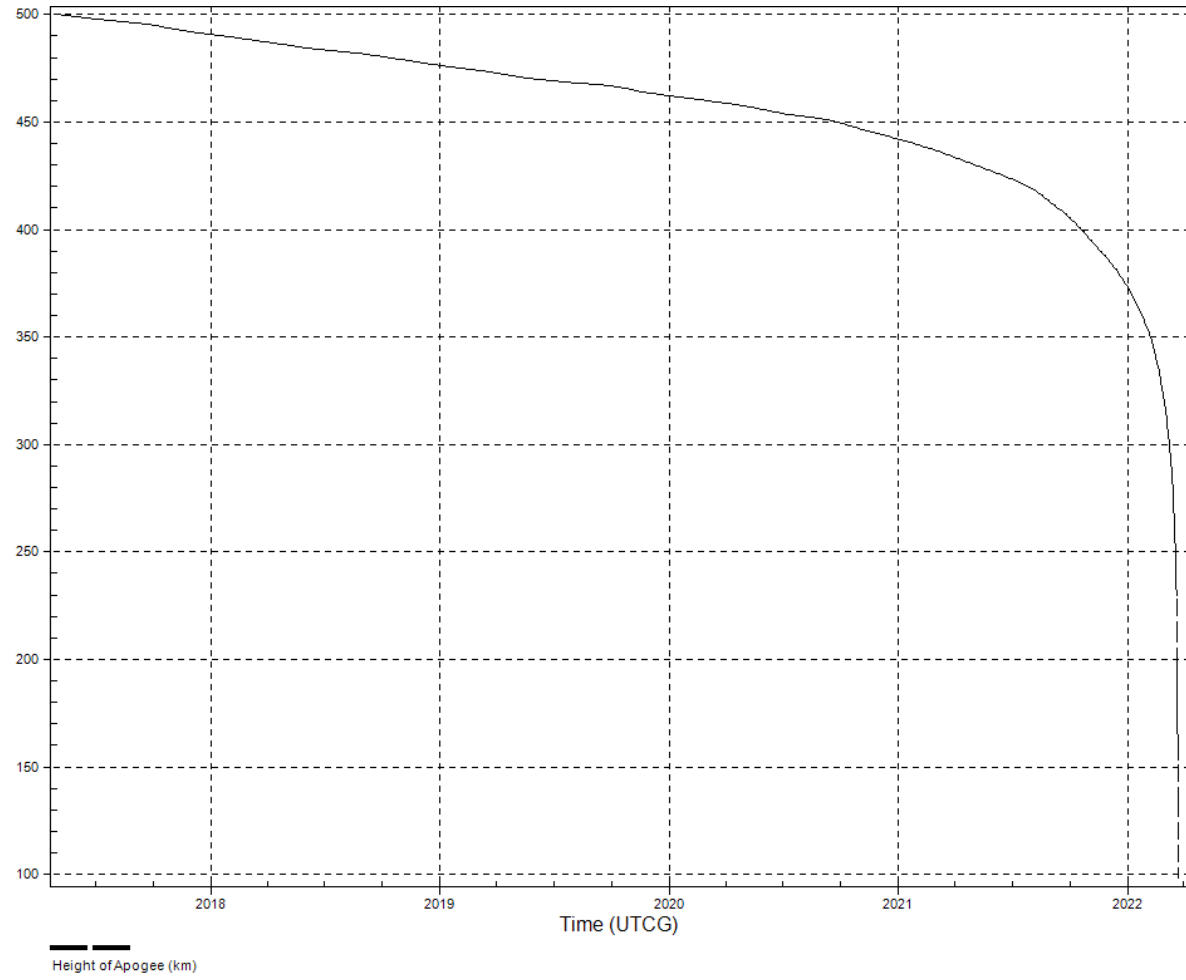
Figure 2.9: Receiver satellite orbit decay from a primary orbit with an assumed mission start in March 2017. Values used: $C_D = 2.22$, mass = 14.92 kg, Area = 0.3 m^2.
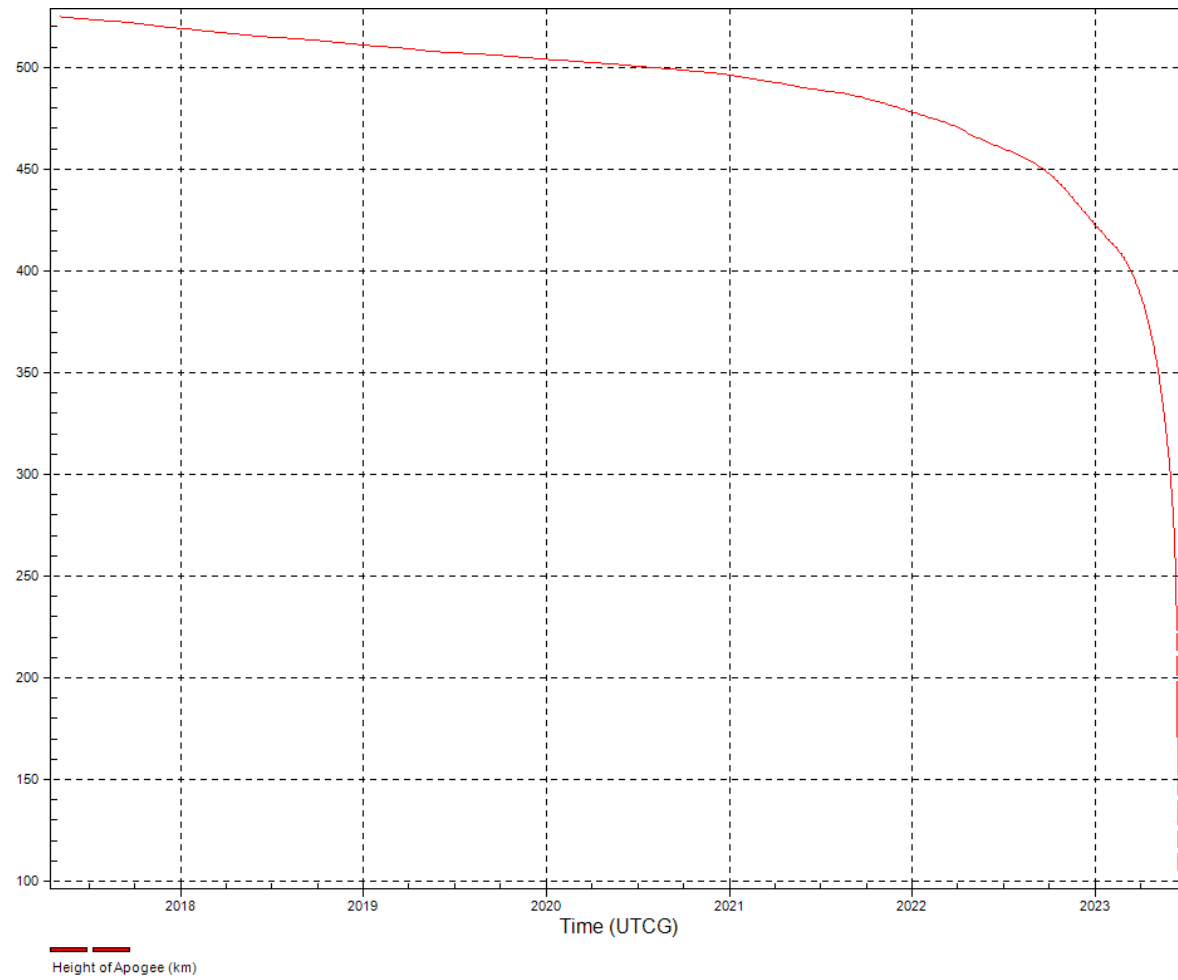
Figure 2.10: Receiver satellite orbit decay from a secondary orbit with an assumed mission start in March 2017. Values used: C_D = 2.22, mass = 14.92 kg, Area = 0.3 m^2.

2.2.3 Swarm Configuration

The general configuration of all the satellites has been presented in the previous section and can be reviewed in figures 2.11 and 2.12. As explained, the general rule of separation is 2.18 degrees between the nodes of the different orbital planes and a 2.18 degree in-track phase offset for the satellites occupying the same orbit.
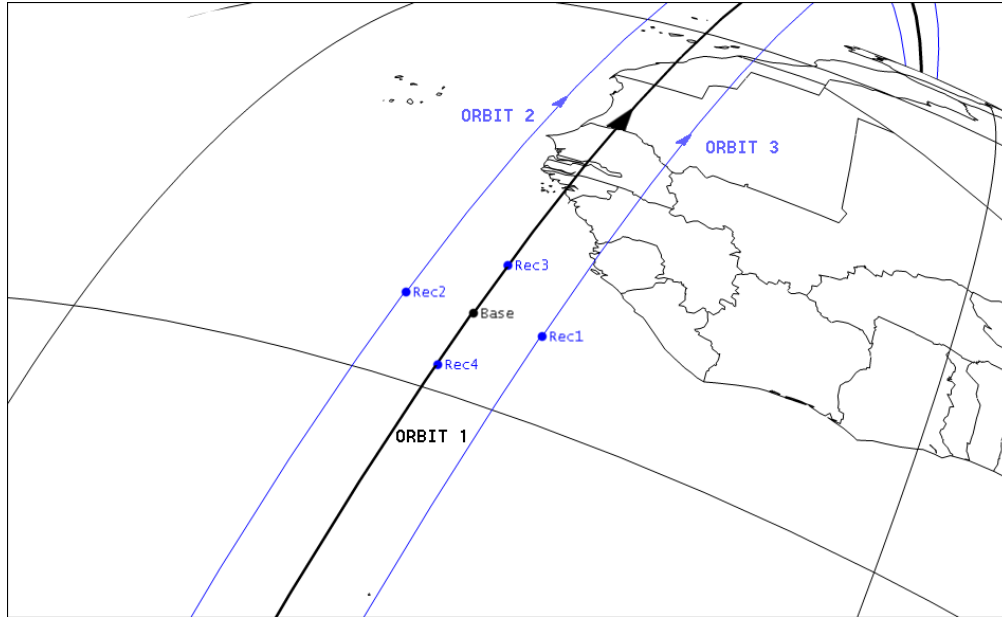

Figure 2.11: Swarm configuration as seen when the emitter (labeled here as Base) crosses its ascending node. Orbit numbers represent the different orbital planes.
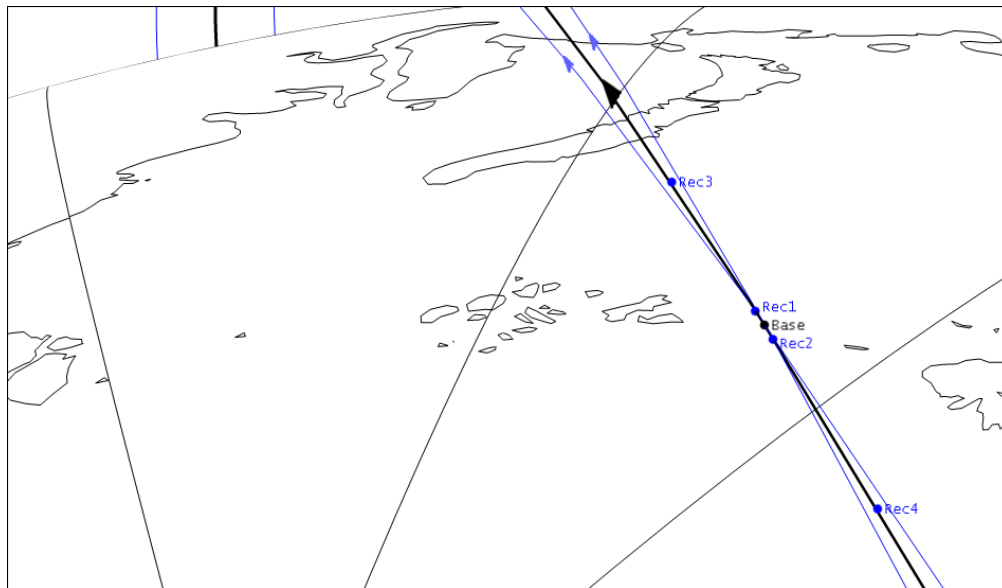

Figure 2.12: Swarm configuration as seen when the orbit planes intersect. In this figure the intersection in ascent is pictured.

A representative ground track can be seen in figure 2.15 on page 24.

From this general configuration several interesting parameters about the formation can be acquired. Please refer to figure 2.13 for a general configuration of geometry for constellations with the same inclinations.
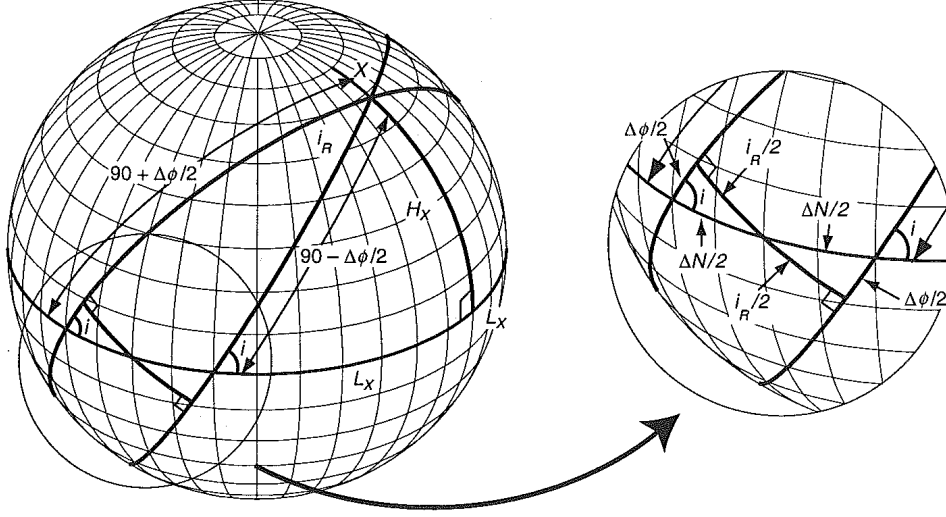

Figure 2.13: Relative geometry between two orbital planes with the same inclination. *Source: [8].*

The large-scale relative motion of two satellites in different orbits is governed by only two key variables: the relative inclination, i_R and relative phase, ϕ_R. The relative inclination is the angle at which the two orbit planes intersect. The relative phase is the angle between the satellites when one intersects the other's orbit. The relative phase is the angular separation of the satellites at the time they intersect each other's orbit plane. This happens four times per orbit. The values of these angles are calculated using the following relations:

$$cos i_R = cos^2 i + sin^2 i cos \Delta N \tag{2.22}$$

$$\phi_R = (T_2 - T_1)n + \Delta\phi \tag{2.23}$$

where

$$\Delta\phi = 180 - 2\phi \tag{2.24}$$

$$tan\phi = \frac{tan(90 - \Delta N/2)}{cos i} \tag{2.25}$$

ΔN is the angular separation at the ascending nodes. Using these equations the relative inclination between Orbit 1 and 2, and 3 and 1 is 2.17 degrees, this corresponds to a separation at the nodes of 261.78 km. The relative inclination between Orbit 2 and 3 is twice this value. The relative phase between the Base and Receiver 1 is 0.1901 (or 22.82 km) as Receiver 1 always crosses Orbit 1 before the emitter satellite. Receiver 2 has the same relative phase with the emitter and trails behind on intersections. The relative phase between satellites in Orbit 2 and 3 is 0.3803 degrees or around 44.6 km.

It is also possible to calculate the maximum and minimum separation angles, λ, using the following relations:

$$sin(\frac{\lambda_{min}}{2}) = sin(\frac{\phi_R}{2})cos(\frac{i_R}{2}) \tag{2.26}$$

$$cos(\frac{\lambda_{max}}{2}) = cos(\frac{\phi_R}{2})cos(\frac{i_R}{2}) \tag{2.27}$$

The maximum and minimum angular separation between any two closest orbital planes then becomes 2.1809 and 0.1901 degrees respectively. The nadir angle can also be calculated. This is the angle between the vector pointing to any other satellite and the Earth center vector. The relations are as following:

$$sin(\eta_{min}) = cos(\lambda_{max}/2) = cos(\phi_R/2)cos(i_R/2) \tag{2.28}$$

$$cos(\eta_{max}) = sin(\lambda_{min}/2) = sin(\phi_R/2)cos(i_R/2) \tag{2.29}$$

The actual values between cross-track satellites are then 89.91 and 88.91 degrees for maximum and minimum respectively. Along-track satellites have a constant nadir angle of 88.91 degrees.

All these values are enough to simulate along and cross-track relative motion between the various satellites. Figure demonstrates the simulation of large scale relative motion between the Base, Receiver 1 and Receiver 2.
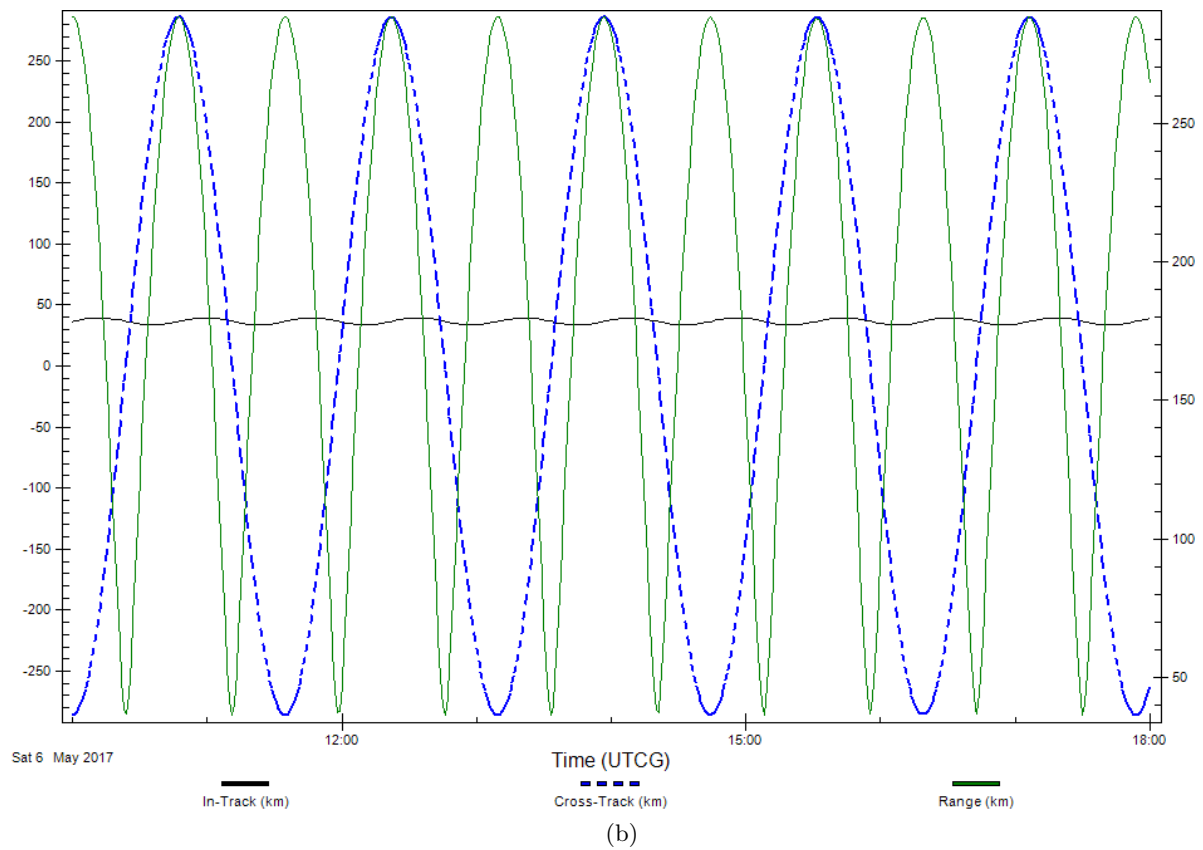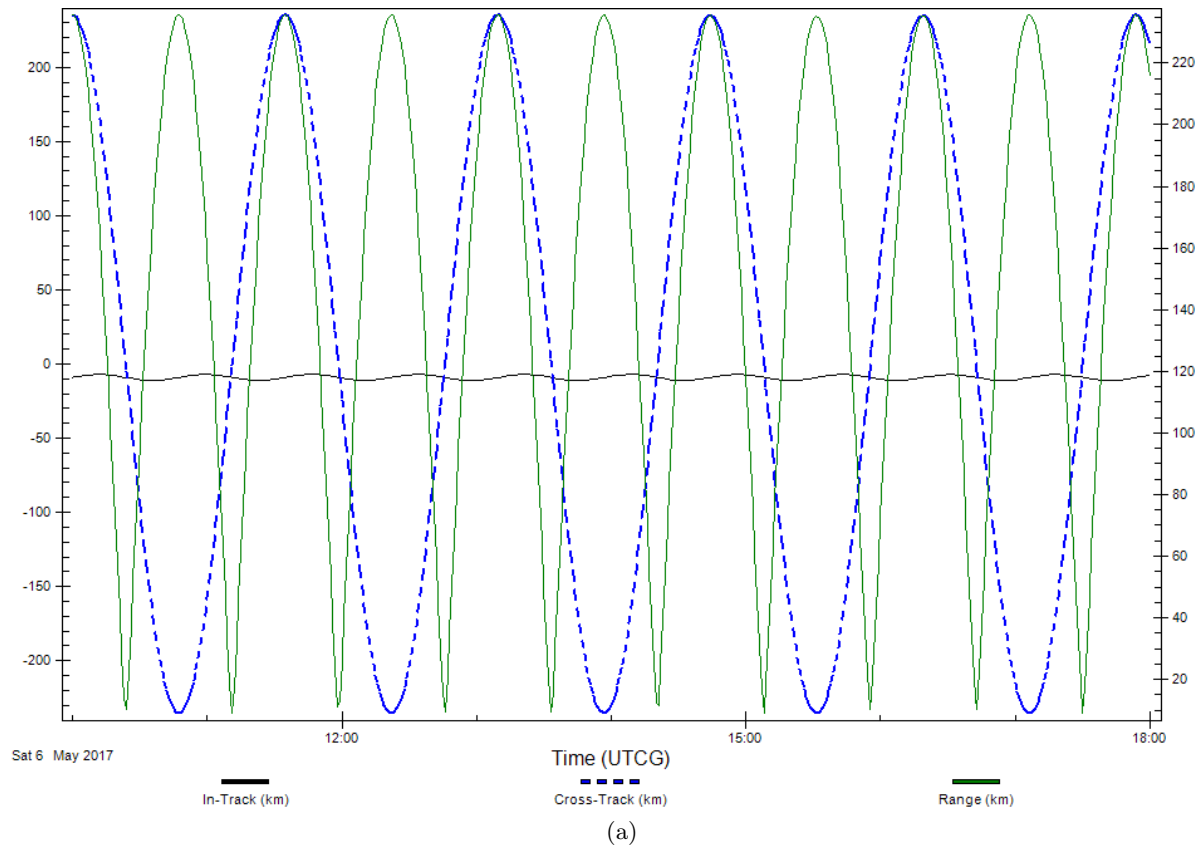
(a)

(b)

Figure 2.14: Large scale relative motion (a) of Receiver 1 w.r.t. Base and (b) of Receiver 2 w.r.t. Base.
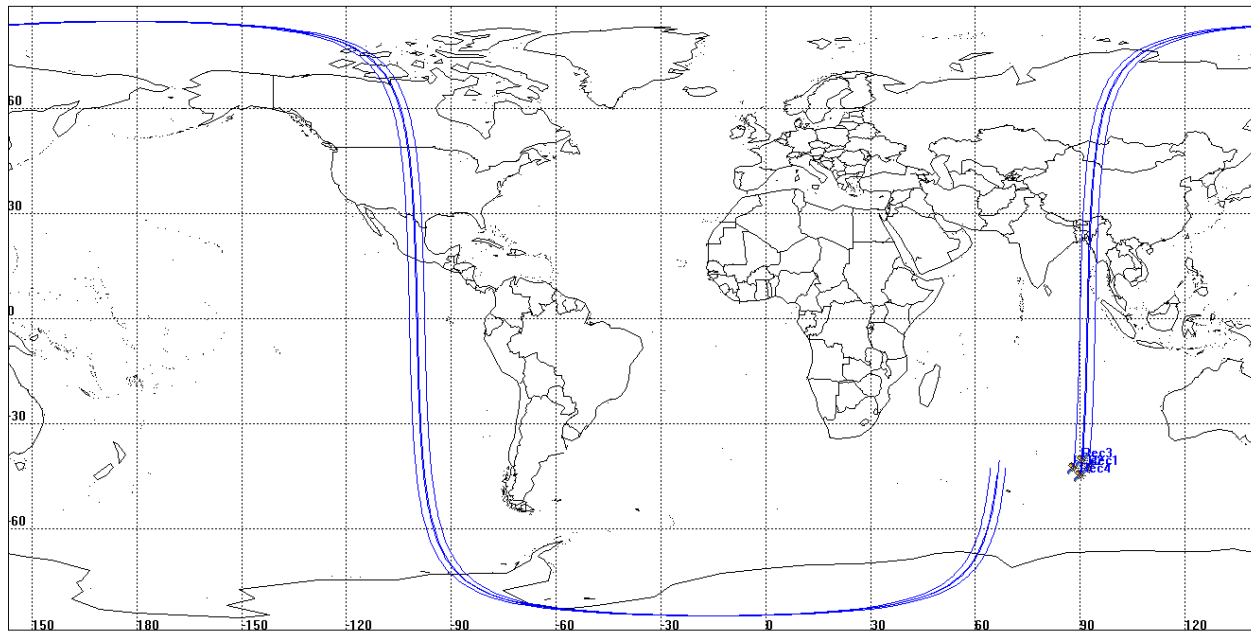
Figure 2.15: A representative ground track of the formation.

2.2.4 Stationkeeping

As mentioned in section 2.2.2.3 the satellites will not require any ΔV for stationkeeping maneuvers. This is because the concept of differential drag will be used to minimize propellant and to make the ballistic coefficients of the satellites more consistent.

The principle works in the following way: the satellites are maintained by following the slowest decaying one. This is known as relative stationkeeping. All the satellites are allowed to decay naturally in sync with that single reference. Since the orbits of every satellite are always known due to accurate navigation, it is possible to analyze decay rates. The satellites are then ordered to adjust the orientation of the solar arrays during eclipse in such a way that differential drag reinstates them into the right positions. This is further made possible due to the fact that not position acquisition but rather position knowledge (and thus correct instrument pointing) is of primary importance to data collection.

This concept has been successfully demonstrated by the ORBCOMM satellites [8]. It is understandable that the process of relative stationkeeping is more difficult to manage, however automated systems and prediction models can be designed to deal with this issue. Such systems however are not discussed here.

2.2.5 Collision Avoidance

bla

2.3 Space Environment and Shielding

Bla

Chapter 3

Sustainable Development Strategy

In this chapter the Sustainable Development Strategy is discussed in the order of production (section 3.1), operations (section 3.2) and End-of-Life (EOL) (section 3.3).

3.1 Production and Logistics

The design is aimed at a swarm of mostly identical satellites. This may allow for series production which is more efficient in terms of resources than a one-of large satellite with a lot of unique components. This also implies that the number of different spare parts could be reduced. Smaller satellites could also use smaller facilities for production and testing.

Transportation can be split up into two parts: transportation to the launch site and the launch from the surface to the final orbit in space. On both occasions the system can again profit from its small size. If the satellites are not launched all together, they can "piggyback" on another satellite's launcher.

Spreading the swarm, i.e. piggybacking using different launchers, has several advantages. First of all, the emissions are lower than in case of a dedicated launcher. Also, if the first satellite fails before the launch of the rest of the swarm, the others can be repaired and thus less resources are wasted.

3.2 Operations

Once in orbit, the satellite's influence on the Earth is very limited. The only real concern is the debris it leaves behind during launch and deployment, which can be dangerous to other satellites orbiting the Earth. However, the deployment mechanism, which is responsible for most of the debris, is not included in this technical feasibility study. Later studies developing the ideas from this feasibility study should take it into account, since more satellites could mean more deployment mechanisms and hence more waste. One aspect that can be dealt with is the efficient use of resources. The swarm can be designed in such a way that if one of the satellites fails a replacement satellite can be sent, whilst any remaining satellites can be reused.

3.3   End of Life

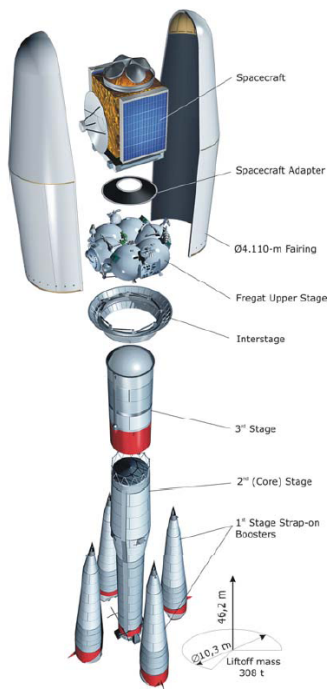Each satellite will be at the end of its life if it cannot perform its function anymore. It is important that after the mission is over all satellites are removed from their orbit and burn up in the atmosphere so that they do not pose any danger to other satellites. Final decommissioning of the swarm will be more complex than for a regular satellite, since every individual satellite has to be decommissioned separately.

Bibliography

[1] Arianespace. *Soyuz from the Guiana Space Center User's Manual*, issue 1 - revision 0 edition, June 2006.

[2] Arianespace. Soyuz launch services overview, 2010.

[3] Charles D. Brown. *Spacraft Mission Design*. American Institute of Aeronautics and Astronautics, Inc., 1992.

[4] Justin Richardson Richard Walker Lindsay Grant Robert K. Henderson Marek Gersbach David Stoppa, Fausto Borghetti and Edoardo Charbon. A 32x32-pixel array with in-pixel photon counting and arrival time measurement in the analog domain. 2009.

[5] EUROCKOT. *EUROCKOT Launch Service Provider User Manual, Chapter 3: General Performance Capabilities*, 4 edition, November 2004.

[6] E. Labonne J. Richardson R. Walker L. Grant R Henderson F. Borghetti D. Stoppa M. Gersbach, Y. Maruyama and E. Charbon. A parallel 32x32 time-to-digital converter array fabricated in a 130 nm imaging cmos technology. 2009.

[7] Cristiano L. Niclass. *Single-Photon Image Sensors in CMOS: Picosecond Resolution for Three-Dimensional Imaging*. PhD thesis, cole Polytechnique Fdrale de Lausanne, 2008.

[8] James R. Wertz. *Mission Geometry; Orbit and Constellation Design and Management*. Microcosm Press and Kluwer Academic Publishers, 2001.

[9] Wiley J. Larson & James R. Wertz, editor. *Space Mission Analysis And Design*. Microcosm Press and Springer, El Segundo, CA (Microcosm Press) & New York, NY (Springer), 3 edition, 2006.

Appendix A

Soyuz-ST Factsheet

Spacecraft

Spacecraft Adapter

Ø4.110-m Fairing

Fregat Upper Stage

Interstage

3rd Stage

2nd (Core) Stage

1st Stage Strap-on Boosters

46,2 m

Ø10,3 m

Liftoff mass 308 t

PAYLOAD FAIRINGS

Fairing	ST
Diameter:	4.110 m
Length:	11.433 m
Mass:	1700 kg
Structure:	Two-half-shell carbon-fiber reinforced plastic
Separation	Mechanical locks/ pneumatic jack/pushers

Interstage	
Mass:	400 kg
Structure:	aluminum skin-stringer

PAYLOAD ADAPTERS

Off-the-shelf devices:

1194SF	(110 kg);
937SF	(45 kg);
1666SF	(100 kg)

FREGAT UPPER STAGE

Size:	3.35-m diameter × 1.50-m height
Inert mass:	950 kg
Propellant:	5350-kg N_2O_4/UDMH
Subsystems:	
Structure:	Structurally stable aluminum alloy 6 spherical tanks/8 cross rods
Propulsion	S5.92
- Thrust	Two mode thrust 19.85/14.00 kN - Vac
- Isp	Two mode thrust 331/316 s - Vac
- Feed system	Pump-fed, open cycle gas generator
- Pressurization	Ghe vaporization
- Burn time / Restart	Up to 900 s / up to 20 controled or depletion burn
Attitude Control	
- pitch, yaw	Main engine translation or eight 50-N hydrazine thrusters
- roll	Four 50-N hydrazine thrusters
Avionics	Inertial 3-axis platform, on-board computer, TM & RF systems, Power
Stage separation:	gas pressure locks/pushers

.	1st STAGE (FOUR BOOSTERS)	2nd STAGE (CORE)	3rd STAGE	
Size:	2.68-m diameter × 19.60-m length	2.95-m diameter × 27.10-m length	2.66-m diameter × 6.70-m length	
Gross/Dry mass:	44 413 kg / 3 784 kg	99 765 kg / 6 545 kg	27 755 kg / 2 355 kg	
Propellant:	27 900-kg LOX 11 260-kg Kerosene	63 800-kg LOX 26 300-kg Kerosene	17 800-kg LOX 7 600 kg Kerosene	
Subsystems:				
Structure	Pressure stabilized aluminium alloy tanks with intertanks skin structure	Pressure stabilized aluminum alloy tanks with intertanks skin structure	Pressure stabilized aluminum alloy tanks with intertanks and rear skin structure	
Propulsion	RD-107A 4-chambers engine,	RD-108A 4-chambers engine,	RD-0110 4-chamber engine (Soyuz 2-1a)	RD-0124 4-chamber engine (Soyuz 2-1b)
- Thrust	838.5 kN – SL; 1021.3 kN –Vac	792.5 kN – SL; 990.2 kN –Vac	297.9 kN (Vac)	297.9 kN (Vac)
- Isp	262 s – SL; 319 s –Vac	255 s – SL; 319 s –Vac	325 s –Vac	359 s (Vac)
- Feed system	pump-fed by hydrogen peroxide (H_2O_2) gas generator	pump-fed by hydrogen peroxide (H_2O_2) gas generator	Pump-fed gas generator, generator's gas blow down through verniers	Multi-stage pump-fed close cycle gas generator
- Pressurization	Liquid nitrogen (N_2)vaporization	Liquid nitrogen (N_2) vaporization	Oxygen vaporization/generator gases	Helium vaporization
- Burn time / Restart	118 s / No – two level thrust throttling	286 s / No – one level thrust throttling	250 s / No	270 s / No
Attitude Control	Two 35-kN vernier thrusters and one aerofin	Four 35-kN vernier thrusters	Four 6-kN vernier thrusters	Each chambers gimbaling in one axis
Avionics	Input/Output units, TM, power	Input/Output units, TM, power	Centralized control system: inertial 3-axis platform, on-board computer, TM & RF system, power	
Stage separation:	Pyronuts/pushers/reaction nozzle	Pyronuts and 3rd stage engine ignition		